# Faraday Discussions

Accepted Manuscript


This manuscript will be presented and discussed at a forthcoming Faraday Discussion meeting. All delegates can contribute to the discussion which will be included in the final volume.

**Register now to attend!** Full details of all upcoming meetings: http://rsc.li/fd-upcoming-meetings

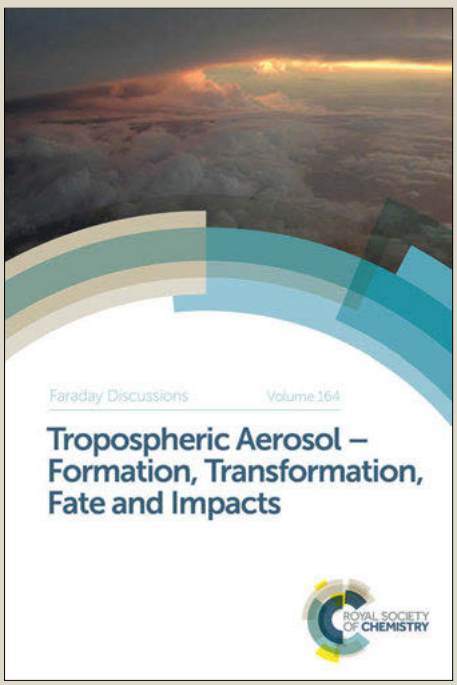


This is an *Accepted Manuscript*, which has been through the Royal Society of Chemistry peer review process and has been accepted for publication.

*Accepted Manuscripts* are published online shortly after acceptance, before technical editing, formatting and proof reading. Using this free service, authors can make their results available to the community, in citable form, before we publish the edited article. We will replace this *Accepted Manuscript* with the edited and formatted *Advance Article* as soon as it is available.

You can find more information about *Accepted Manuscripts* in the Information for Authors.

Please note that technical editing may introduce minor changes to the text and/or graphics, which may alter content. The journal's standard Terms & Conditions and the Ethical guidelines still apply. In no event shall the Royal Society of Chemistry be held responsible for any errors or omissions in this *Accepted Manuscript* or any consequences arising from the use of any information it contains.


ROYAL SOCIETY OF CHEMISTRY

www.rsc.org/faraday_d

CREATED USING THE RSC LaTeX PCCP ARTICLE TEMPLATE – SEE www.rsc.org/electronicfiles FOR DETAILS
PAPER www. rsc.org/faraday_d | Faraday Discussions

# High-order harmonic spectroscopy for molecular imaging of polyatomic molecules

**M. Negro,[a] M. Devetta,[a] D. Faccialá,[b] S. De Silvestri,[b] C. Vozzi[a*] and S. Stagira,[b]**

***Received Xth XXXXXXXXXX 20XX, Accepted Xth XXXXXXXXX 20XX***
***First published on the web Xth XXXXXXXXXX 200X***
**DOI: 10.1039/c000000x**

High-order harmonic generation is a powerful and sensitive tool for probing atomic and molecular structures, combining in the same measurement an unprecedented attosecond temporal resolution with a high spatial resolution, of the order of the angstrom. Imaging of the outermost molecular orbital by high-order harmonic generation has been limited for a long time to very simple molecules, like nitrogen. Recently we demonstrated a technique that overcame several of the issues that have prevented the extension of molecular orbital tomography to more complex species, showing that molecular imaging can be applied to a triatomic molecule like carbon dioxide. Here we report on the application of such technique to nitrous oxide ($N_2O$) and acetylene ($C_2H_2$). This result represents a first step towards the imaging of fragile compounds, a category which includes ~~the~~ most of the fundamental biological molecules.

## 1 Introduction

High order harmonic generation (HHG) occurs when atoms or molecules exposed to an intense femtosecond laser pulse are ionized by tunneling. The freed electron is then accelerated in the external electric field. Because of the periodic oscillation of the laser field, the electron is brought back to the parent ion where it may recombine emitting an XUV photon[1]. This XUV radiation has been shown to contain information on the electronic structure of the emitting molecule and on its internal dynamics. Attosecond nuclear[2] and electronic dynamics[3,4] have been extracted from HHG in simple molecules and spectral features in the harmonic emission have been related to the molecular electronic structure and have been used for imaging the highest occupied molecular orbital (HOMO).

The idea of exploiting HHG for the tomographic reconstruction of molecular orbitals was first introduced by Itatani et al. in 2004 for the nitrogen molecule[5]. Since then, numerous experiments have been realized, addressing the role of

[a] *Istituto di Fotonica e Nanotecnologie - CNR, 20133 Milan, Italy*
[b] *Dipartimento di Fisica - Politecnico di Milano, 20133 Milan, Italy*
* corresponding author: caterina.vozzi@ifn.cnr.it

the HOMO in the harmonic spectral intensity[6,7], in the molecular-frame photoionization[8] and in the subsequent attosecond XUV emission[9], as well as in the polarization state of the emitted radiation[10]. The dependence of the HHG process on the HOMO structure has also been exploited for the characterization in the time domain of the rotational[11] and vibrational[12] molecular excitations.

All these studies rely on two major assumptions: (i) the molecular HHG is dominated by the HOMO structure; (ii) the relationship between molecular structure and emitted XUV spectrum is simple and completely captured by the Strong Field Approximation (SFA), i.e. the electron quiver motion is not perturbed by the Coulomb potential of the ion.

Both these assumptions have been recently put into question. Recent experiments enlightened the role of multiple orbital contributions to HHG emission[3,4]. Furthermore, the influence of the Coulomb field of the parent ion in the generation of high order harmonics from molecules has been considered as a serious hindrance to a clear HOMO reconstruction[13]. These assumptions should then be overtaken to perform molecular tomography to more complex species.

Besides these two more fundamental obstacles, there are also additional, more technical difficulties. In order to retrieve the HOMO structure, one has to record the XUV harmonic spectra for different molecular orientations with respect to the laser field. Hence, it is necessary to fix the molecular orientation in space and change the polarization direction of the HHG-driving field[5]. Laser-assisted molecular alignment is a widespread technique able to accomplish this task[14], but the molecular alignment achieved in this way is not ideal. Hence the experimental results and the corresponding HOMO tomography are affected by angular averaging effects. Moreover, in the case of non-linear molecules, the tomographic procedure requires to fix two or three angular coordinates of the molecule under investigation. For instance, the study of linear polar molecules requires to fix the head-tail direction in space. The feasibility of laser assisted molecular orientation has been recently demonstrated[15] and exploited in HHG spectroscopy[16–18], but no direct application to molecular imaging has been yet realized.

The amount of information that can be extracted from the harmonic emission depends on the spectral extension of the XUV radiation, that is known to scale with the so-called cut-off law: $E_{max} = I_p + 3.17U_p$, where $I_p$ is the ionization potential of the molecule and $U_p$ is the ponderomotive energy of the electron in the laser field. This poses another important problem when HHG molecular imaging is extended to species with low ionization potential (i.e. all organic molecules, and in particular those having important biological functions) as the extension emission spectrum is reduced. Since $U_p \propto \lambda^2 I$, where I is the peak intensity and $\lambda$ the wavelength of the driving laser pulse, the emission cut-off may be extended by both increasing the field intensity or the laser wavelength. In this respect, standard Ti:Sapphire laser sources generally used in HHG are not ideal candidates for tomography in fragile molecules, since the intense optical fields needed completely ionize the molecule before a well-developed XUV spectrum is generated.

To overcome the limitations posed by ionization saturation, the exploitation of mid-infrared driving sources has been demonstrated to be a powerful tool to extend harmonic emission far in the XUV[19–23].

 

With a mid-IR source[24] we recently demonstrated that it is possible to extend the spectral investigation in carbon dioxide beyond 100 eV in the absence of multielectron effects, thus avoiding any ambiguity in the reconstructed wavefunction. In addition, by exploiting an all-optical non-interferometric technique, it was possible to trace both the spectral intensity and phase of high order harmonics generated by single molecules as a function of emitted photon energy and molecular angular orientation, without averaging effects. Furthermore, the tomographic procedure was generalized in order to take into account the Coulomb potential seen by the re-colliding electron wavepacket[25].

In this work, we extend that approach to more complex molecules, such as $N_2O$ and $C_2H_2$ pointing out some strengths and weaknesses of this investigation technique.

## 2 Experimental ~~Results~~ Setup

We exploited an optical parametric amplifier (OPA) pumped by an amplified Ti:sapphire laser system (60 fs, 20 mJ, 800 nm). The OPA is based on difference frequency generation and provides driving pulses with 1450 nm central wavelength, pulse duration of 20 fs and pulse energy of 1.2 mJ[24]. High harmonics were generated by focusing the mid-IR pulse in a supersonic gas jet under vacuum, due to the strong absorption exhibited by air in the XUV spectral region. The molecules in the jet were impulsively aligned with a portion of the fundamental 800-nm beam which was spectrally broadened by optical filamentation in an argon-filled gas cell and temporally stretched up to 100 fs by propagation through a glass plate. Such duration is required for achieving a good alignment of the molecular sample. In our experimental setup, driving and aligning pulse were collinear and their polarizations were parallel. The delay between the two pulses was adjusted by means of a fine-resolution translation stage. The XUV radiation was acquired by means of a flat-field spectrometer and a multi-channel plate detector coupled to a CCD camera[26].

## 3 Results

Harmonic spectra were acquired in $N_2O$ and $C_2H_2$ as a function of the delay $\tau$ between the aligning and driving pulse around the first rotational half revival ($\tau_{N_2O} = 19.95$ ps and $\tau_{C_2H_2} = 7.08$ ps). The results are shown in figure 1(a) and 2(a) for $N_2O$ and $C_2H_2$ respectively. Figures 1(b) and 2(b) show the corresponding calculated alignment factor for the experimental conditions.

In both molecules, the sequence of harmonic spectra shows a strong modulation with the delay $\tau$ that can be ascribed to the dependence of harmonic yield on the molecular orbital structure. In particular, a reduction of the harmonic emission can be observed for the delay corresponding to the maximum of the alignment factor and an enhancement of the harmonic yield appears for the minimum of the alignment factor. A major difference between the two cases is the presence of a region of harmonic enhancement at high photon energy, that appears in $N_2O$ at maximum alignment.

These effects can be naively interpreted in terms of two-center interference occurring in the re-collision step[7,27]. If one consider a diatomic homo-nuclear

molecule with a symmetric electronic state with respect to the nuclei exchange and assumes the re-colliding electron as a plane wave, the condition for constructive interference reads $R\cos(\theta) = n\lambda_B$, where $R$ is the internuclear separation, $\theta$ is the angle between the molecular axis and the electron wave-vector, $n$ is an integer number and $\lambda_B$ is the de Broglie wavelength associated to the re-colliding electron wave-packet. Similarly the condition for destructive interference is $R\cos(\theta) = (n+1/2)\lambda_B$ and the first destructive interference occurs for $n = 0$. The conditions become reversed for molecules with antisymmetric electronic structure.

This concept can be extended to the molecules subject of our investigation. The acetylene molecule has a symmetric $\pi$ HOMO in which the separation between the carbon atoms is $R_{C\equiv C} = 1.2$ Å. This is the distance that should be considered for the evaluation of the interference condition. The $N_2O$ HOMO does not have a clear symmetry, however in our experimental condition the harmonic spectra are acquired in aligned molecules and correspond to the average between the two possible orientation. The resulting signal can be interpreted in terms of emission from an effective molecular orbital similar to the anti-symmetric $\pi$ orbital of $CO_2$. In this view the overall length of this "effective" orbital is $R_{N_2O} = 2.3$ Å. Since $R_{N_2O} \approx 2R_{C\equiv C}$, a destructive interference occurs in the same spectral region for both molecules, corresponding to $n = 1$ for $N_2O$ and $n = 0$ for $C_2H_2$.

Figures 1(a) and 2(a) show two peculiar advantages related to the exploitation of mid-IR driving pulses for HHG. Indeed the harmonic cutoff extension related to the increase in the ponderomotive energy with respect to standard Ti:sapphire sources allows the observation of spectral features as the harmonic enhancement for high photon energy visible in $N_2O$ in correspondence of the revival peak. In the framework of the above mentioned two-center model, this feature can be attributed to the appearance of constructive interference in that spectral region. Moreover, for the same emitted photon energy, mid-IR driving wavelengths require a lower pulse peak intensity thus reducing the ionization saturation in species with relatively low ionization potential, such as $C_2H_2$ ($I_P = 11.4$ eV).

## 4 Reconstruction of Single Molecule XUV Emission

From the experimental data reported in figures 1(a) and 2(a) it is possible to retrieve structural information on the target molecule following the approach introduced by Vozzi et al.[25]. Figures 3(a) and 4(a) show the same experimental results presented in figures 1(a) and 2(a), in which the harmonic structure due to the periodic re-collision of the electron wave-packet has been filtered out. These results have been exploited for the reconstruction of the XUV field emitted from a single molecule and projected on the polarization direction of the aligning field as a function of the angle between the molecular axis and the driving polarization direction. The reconstruction is based on a combination of a phase-retrieval algorithm and a Kaczmarz algorithm[28]. The main idea behind this approach is that the macroscopic XUV emission is the coherent superposition of the XUV field emitted by all molecules weighted with their angular distribution. This distribution changes along the revival in a predictable way, hence the sequence of harmonic emission contains enough information for the reconstruction of the har-

 

monic electric field in amplitude and phase.

The result of this reconstruction is shown in figure 5 for $N_2O$ and in figure 6 for $C_2H_2$. In both figures, panel (a) reports the amplitude of the XUV field and panel (b) shows the corresponding phase. In $N_2O$ there is a clear phase jump of about 2 rad, that changes its position with photon energy and molecular alignment. This phase jump corresponds to a minimum in the XUV amplitude and its position is quite in good agreement with the prediction of the naive two-center model introduced above, which is shown as a dashed line in the figure. It is worth noting that the reconstruction technique is based on the interference of XUV emission from different molecular orientations, thus the phase can be retrieved as a function of $\theta$ at fixed XUV photon energy. In order to retrieve the phase relationship between contributions at neighboring energies, it is necessary to introduce an a priori condition that can be derived from theoretical considerations or experimental measurements. In the case of $N_2O$ we imposed a flat spectral phase of the macroscopic harmonic emission for the delay corresponding to the molecular anti-alignment. This condition was chosen in analogy with the $CO_2$ case[25], due to the similarity between the two HOMOs as discussed in the previous section. The results of this assumption can be observed in figure 3, where the reconstructed amplitude (b) and phase (c) of the macroscopic XUV emission from $N_2O$ are reported. The retrieved amplitude is in good agreement with the experimental data (figure 3(a)). The phase of the macroscopic emission shows a steep change of about 2 rad around 50 eV at the delay $\tau$ corresponding to the maximum alignment.

In the case of $C_2H_2$ we followed the same approach in the retrieval procedure. We imposed in this case a flat spectral phase for the macroscopic harmonic emission at the delay $\tau$ corresponding to the molecular alignment. This assumption was necessary in order to complete the retrieval procedure, but it is arbitrary and not supported by theoretical models; it could be however improved by changing the retrieving condition according to an experimental spectral phase measurement. This kind of experiment can be performed for example by RABBIT technique at a given alignment delay[9]. The retrieved single molecule XUV emission in $C_2H_2$, shown in figure 6, is very different from the one reported for $N_2O$. In particular a strong contribution comes from molecules with perpendicular orientation with respect to the driving field polarization direction. In the retrieved phase (figure 6(c)) two phase jumps are clearly observed. The first one appears for small alignment angles and roughly follows the prediction of the two-center model. The second jump appears at large alignment angles and may be attributed to the shape of the HOMO seen by the re-colliding electron. However, since the reconstruction is based on the arbitrary assumption of flat macroscopic spectral phase at the alignment delay, the retrieved outcomes should be considered preliminary. In spite of this, the retrieved macroscopic XUV amplitude (figure 4(b)) is in fair agreement with the experimental results.

## 5 Molecular Orbital Tomography

The results reported in the previous section can be used for the two-dimensional reconstruction of ----- molecular orbitals, following the tomographic procedure proposed by Itatani et al.[5] and extended by Vozzi et al.[25]. However to proceed

with this tomographic reconstruction, it is necessary to rule out the occurrence of multi-electron effects in HHG. A simple experimental procedure to check whether spectral modulations in harmonic emission are due to multi-electron effects is to change the driving field intensity. As shown by Smirnova et al.[3], one expects all the features due to multi-electron effects to shift with the driving field intensity. Figure 7 shows harmonic spectra acquired in aligned $N_2O$ for a delay $\tau$ corresponding to the maximum of the alignment for different values of the driving intensity. The spectral minimum associated to the phase change retrieved in figure 5(b) appears always around 55 eV and does not shift with the intensity. This behavior guarantees that the main spectral features in the harmonic emission are mainly dictated by the HOMO structure. This consistency check allowed us to exploit the retrieved single molecule harmonic emission for the reconstruction of $N_2O$ orbital. The result is shown in figure 8(a). Figure 8(b) shows the $N_2O$ orbital calculated with a quantum chemistry program[29]. Even if the overall dimension of the molecular orbital is well reproduced, the asymmetry of this orbital is very clear and cannot be addressed by the tomographic reconstruction, since in the experiment the molecules were aligned but not oriented. Another departure of the retrieved orbital with respect to the calculated one is the presence of side lobes, that can be attributed to the limited working range of the XUV spectrometer used in these experiments. Since there is a correspondence between the energy range of harmonic emission and the spatial frequency domain, the limited spectral range collectible in the experiment corresponds to a spatial filtering in the Fourier domain, which gives raise to such lobes. These observations are further confirmed by figure 8(c), which shows the calculated HOMO corresponding to the average between the two possible orientations of $N_2O$ molecular axis and takes into account the limited spectral bandwidth available in the experiment. The features of this fictitious orbital are in very good agreement with the reconstruction of figure 8(a). It is worth nothing that such limitations can be overcome by extending the acquired spectral range over all the XUV emission and by exploiting all-optical impulsive techniques for orientation of polar molecules, such the one demonstrated by Frumker et al.[16,17].

Differently from the case of $N_2O$, in $C_2H_2$ it is not possible to easily rule out the multi-electron contributions. Because of the smaller cutoff energy, the experimental approach applied in the case of $N_2O$ for the exclusion of multi-electron contribution is not feasible. Nevertheless the application of tomographic approach to the single molecule emission maps shown in figure 6 provides interesting results. We show in figure 9(a) the retrieved $C_2H_2$ HOMO. Also in this case, a comparison with the result calculated with a quantum chemistry program (see figure 9(b)) shows a good agreement in the overall shape of the orbital. Again the additional lobes are related to the limited harmonic range detected in the experimental acquisition, as can be seen in figure 9(c) where the orbital is calculated taking into account the spectral filtering.

## 6 Conclusions

Since the pioneering work of Itatani et al. on molecular orbital imaging, the impressive advances in laser technologies gave the access to new mid-IR sources for driving HHG and pushing the harmonic emission far towards the soft-X ray

 

range. These sources allowed the application of HHG spectroscopy to fragile molecules as hydrocarbons, which play as prototypes for the study of ubiquitous phenomena in chemistry and material science. In this work we showed the application of molecular orbital reconstruction based on HHG to non-trivial samples, such as $N_2O$ and $C_2H_2$. These results, though requiring further improvements, demonstrate the capability of molecular orbital tomography and represent the first step towards the imaging of dynamical processes in complex molecules.

## Acknowledgements

The research leading to these results has received funding from LASERLAB-EUROPE (grant agreement n 284464, EC Seventh Framework Programme), from ERC Starting Research Grant UDYNI (grant agreement n 307964, EC Seventh Framework Programme) and from the Italian Ministry of Research and Education (ELI project - ESFRI Roadmap).

## References

1 P. B. Corkum, Phys. Rev. Lett., 1993, **71**, 1994–1997.
2 S. Baker, J. Robinson, C. Haworth, H. Teng, R. Smith, C. Chirila, M. Lein, J. Tisch and J. Marangos, SCIENCE, 2006, **312**, 424–427.
3 O. Smirnova, Y. Mairesse, S. Patchkovskii, N. Dudovich, D. Villeneuve, P. Corkum and M. Y. Ivanov, NATURE, 2009, **460**, 972–977.
4 S. Haessler, J. Caillat, W. Boutu, C. Giovanetti-Teixeira, T. Ruchon, T. Auguste, Z. Diveki, P. Breger, A. Maquet, B. Carre, R. Taieb and P. Salieres, NATURE PHYSICS, 2010, **6**, 200–206.
5 J. Itatani, J. Levesque, D. Zeidler, H. Niikura, H. Pepin, J. Kieffer, P. Corkum and D. Villeneuve, NATURE, 2004, **432**, 867–871.
6 T. Kanai, S. Minemoto and H. Sakai, NATURE, 2005, **435**, 470–474.
7 C. Vozzi, F. Calegari, E. Benedetti, J. Caumes, G. Sansone, S. Stagira, M. Nisoli, R. Torres, E. Heesel, N. Kajumba, J. Marangos, C. Altucci and R. Velotta, PHYSICAL REVIEW LETTERS, 2005, **95**, 153902.
8 A.-T. Le, R. R. Lucchese, M. T. Lee and C. D. Lin, Phys. Rev. Lett., 2009, **102**, 203001.
9 W. Boutu, S. Haessler, H. Merdji, P. Breger, G. Waters, M. Stankiewicz, L. J. Frasinski, R. Taieb, J. Caillat, A. Maquet, P. Monchicourt, B. Carre and P. Salieres, NATURE PHYSICS, 2008, **4**, 545–549.
10 J. Levesque, Y. Mairesse, N. Dudovich, H. Pépin, J.-C. Kieffer, P. B. Corkum and D. M. Villeneuve, Phys. Rev. Lett., 2007, **99**, 243001.
11 K. Miyazaki, M. Kaku, G. Miyaji, A. Abdurrouf and F. H. M. Faisal, Phys. Rev. Lett., 2005, **95**, 243903.
12 W. Li, X. Zhou, R. Lock, S. Patchkovskii, A. Stolow, H. C. Kapteyn and M. M. Murnane, SCIENCE, 2008, **322**, 1207–1211.
13 Z. B. Walters, S. Tonzani and C. H. Greene, JOURNAL OF PHYSICAL CHEMISTRY A, 2008, **112**, 9439–9447.
14 H. Stapelfeldt and T. Seideman, REVIEWS OF MODERN PHYSICS, 2003, **75**, 543–557.
15 S. De, I. Znakovskaya, D. Ray, F. Anis, N. G. Johnson, I. A. Bocharova, M. Magrakvelidze, B. D. Esry, C. L. Cocke, I. V. Litvinyuk and M. F. Kling, Phys. Rev. Lett., 2009, **103**, 153002.
16 E. Frumker, C. T. Hebeisen, N. Kajumba, J. B. Bertrand, H. J. Woerner, M. Spanner, D. M. Villeneuve, A. Naumov and P. B. Corkum, PHYSICAL REVIEW LETTERS, 2012, **109**, 113901.
17 E. Frumker, N. Kajumba, J. B. Bertrand, H. J. Wörner, C. T. Hebeisen, P. Hockett, M. Spanner, S. Patchkovskii, G. G. Paulus, D. M. Villeneuve, A. Naumov and P. B. Corkum, Phys. Rev. Lett., 2012, **109**, 233904.
18 M. Spanner, S. Patchkovskii, E. Frumker and P. Corkum, Phys. Rev. Lett., 2012, **109**, 113001.

19 E. J. Takahashi, T. Kanai, K. L. Ishikawa, Y. Nabekawa and K. Midorikawa, Phys. Rev. Lett., 2008, **101**, 253901.

20 C. Vozzi, R. Torres, M. Negro, L. Brugnera, T. Siegel, C. Altucci, R. Velotta, F. Frassetto, L. Poletto, P. Villoresi, S. De Silvestri, S. Stagira and J. P. Marangos, APPLIED PHYSICS LETTERS, 2010, **97**, 241103.

21 C. Vozzi, F. Calegari, M. Negro, F. Frassetto, L. Poletto, G. Sansone, P. Villoresi, M. Nisoli, S. De Silvestri and S. Stagira, Journal of Modern Optics, 2010, **57**, 1008–1013.

22 C. Vozzi, F. Calegari, F. Frassetto, M. Negro, L. Poletto, G. Sansone, P. Villoresi, M. Nisoli, S. Silvestri and S. Stagira, Laser Physics, 2010, **20**, 1019–1027.

23 T. Popmintchev, M.-C. Chen, D. Popmintchev, P. Arpin, S. Brown, S. Ališauskas, G. Andriukaitis, T. Balčiunas, O. D. Mücke, A. Pugzlys, A. Baltuška, B. Shim, S. E. Schrauth, A. Gaeta, C. Hernández-García, L. Plaja, A. Becker, A. Jaron-Becker, M. M. Murnane and H. C. Kapteyn, Science, 2012, **336**, 1287–1291.

24 C. Vozzi, F. Calegari, E. Benedetti, S. Gasilov, G. Sansone, G. Cerullo, M. Nisoli, S. De Silvestri and S. Stagira, OPTICS LETTERS, 2007, **32**, 2957–2959.

25 C. Vozzi, M. Negro, F. Calegari, G. Sansone, M. Nisoli, S. De Silvestri and S. Stagira, NATURE PHYSICS, 2011, **7**, 822–826.

26 L. Poletto, G. Tondello and P. Villoresi, REVIEW OF SCIENTIFIC INSTRUMENTS, 2001, **72**, 2868–2874.

27 M. Lein, N. Hay, R. Velotta, J. Marangos and P. Knight, PHYSICAL REVIEW A, 2002, **66**, 023805.

28 C. Popa and R. Zdunek, MATHEMATICS AND COMPUTERS IN SIMULATION, 2004, **65**, 579–598.

29 DALTON, a molecular electronic structure program Release 2.0 (2005) see http://www.kjemi.uio.no/software/dalton/dalton.html.




 

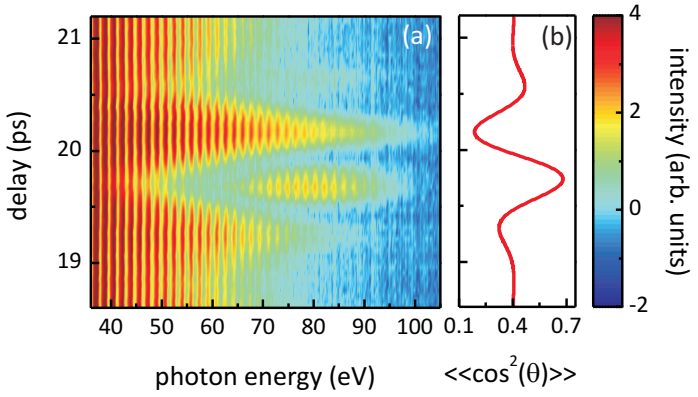


**Fig. 1** (a) Sequence of harmonic spectra measured in $N_2O$ as a function of emitted photon energy and delay between the aligning and the driving pulse (log scale). (b) Calculated alignment factor for $N_2O$ in the experimental conditions (rotational temperature 75 K, aligning pulse duration 100 fs, aligning pulse intensity $3.32 \times 10^{13}$ W/cm$^2$).

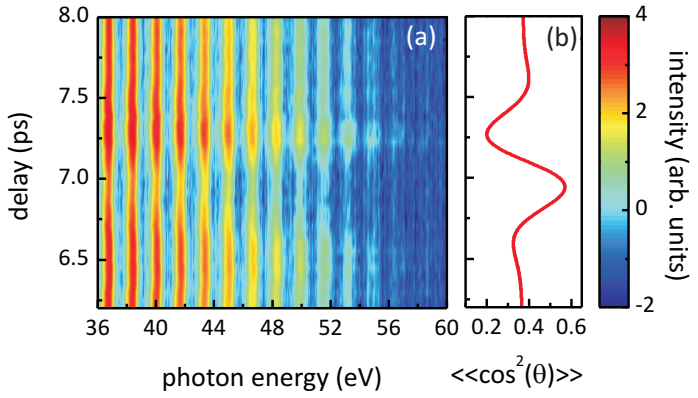


**Fig. 2** (a) Sequence of harmonic spectra measured in $C_2H_2$ as a function of emitted photon energy and delay between the aligning and the driving pulse (log scale). (b) Calculated alignment factor for $C_2H_2$ in the experimental conditions (rotational temperature 75 K, aligning pulse duration 100 fs, aligning pulse intensity $2.16 \times 10^{13}$ W/cm$^2$).

**Fig. 3** (a) Sequence of XUV spectra measured in $N_2O$ as a function of emitted photon energy and delay between the aligning and the driving pulse; the harmonic structure has been filtered out. Retrieved macroscopic harmonic emission amplitude (b) and phase (c) corresponding to the data reported in (a).



 

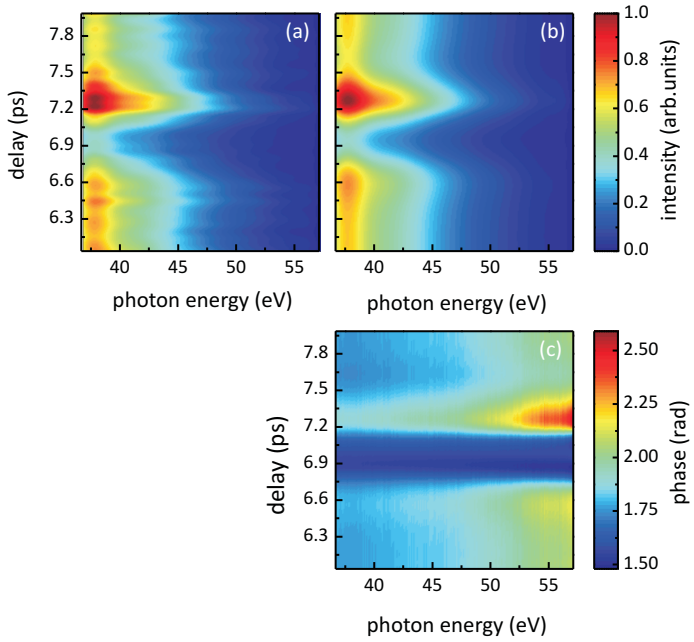


**Fig. 4** (a) Sequence of XUV spectra measured in $C_2H_2$ as a function of emitted photon energy and delay between the aligning and the driving pulse; the harmonic structure has been filtered out. Retrieved macroscopic harmonic emission amplitude (b) and phase (c) corresponding to the data reported in (a).

**Fig. 5** Retrieved single molecule XUV emission map in $N_2O$ as a function of emitted photon energy and the angle between the molecular axis and the aligning beam polarization direction in amplitude (a) and phase(b). Dashed lines show the position of the destructive interference predicted by the two-center model.

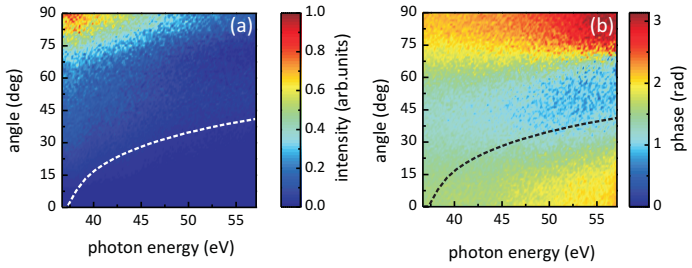


**Fig. 6** Retrieved single molecule XUV emission map in $C_2H_2$ as a function of emitted photon energy and the angle between the molecular axis and the aligning beam polarization direction in amplitude (a) and phase(b). Dashed lines show the position of the destructive interference predicted by the two-center model.

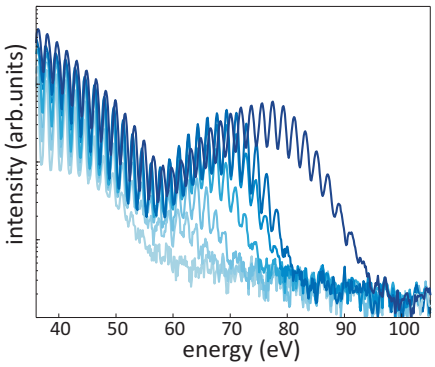


**Fig. 7** Harmonic spectra generated in $N_2O$ at the delay $\tau$ corresponding to the maximum molecular alignment for several driving peak intensities I between 1 and $1.7 \times 10^{14}$ W/cm$^2$.

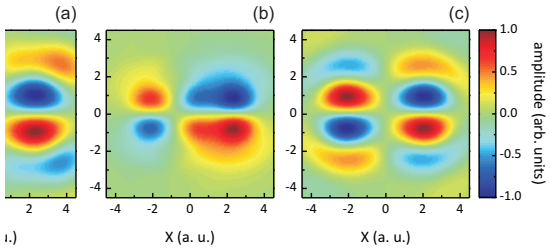


**Fig. 8** (a) Highest occupied molecular orbital of $N_2O$ as retrieved from the single molecule XUV emission map. (b) Highest occupied molecular orbital of $N_2O$ calculated with a quantum chemistry program[29]. (c) $N_2O$ HOMO calculated averaging over the two possible orientations of the molecular axis and considering the filtering in spectral domain corresponding to the experimental conditions.

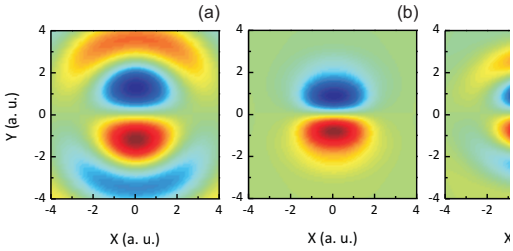


**Fig. 9** a) Highest occupied molecular orbital of $C_2H_2$ as retrieved from the single molecule XUV emission map. (b) Highest occupied molecular orbital of $C_2H_2$ calculated with a quantum chemistry program[29]. (c) $C_2H_2$ HOMO calculated considering the filtering in spectral domain corresponding to the experimental conditions.